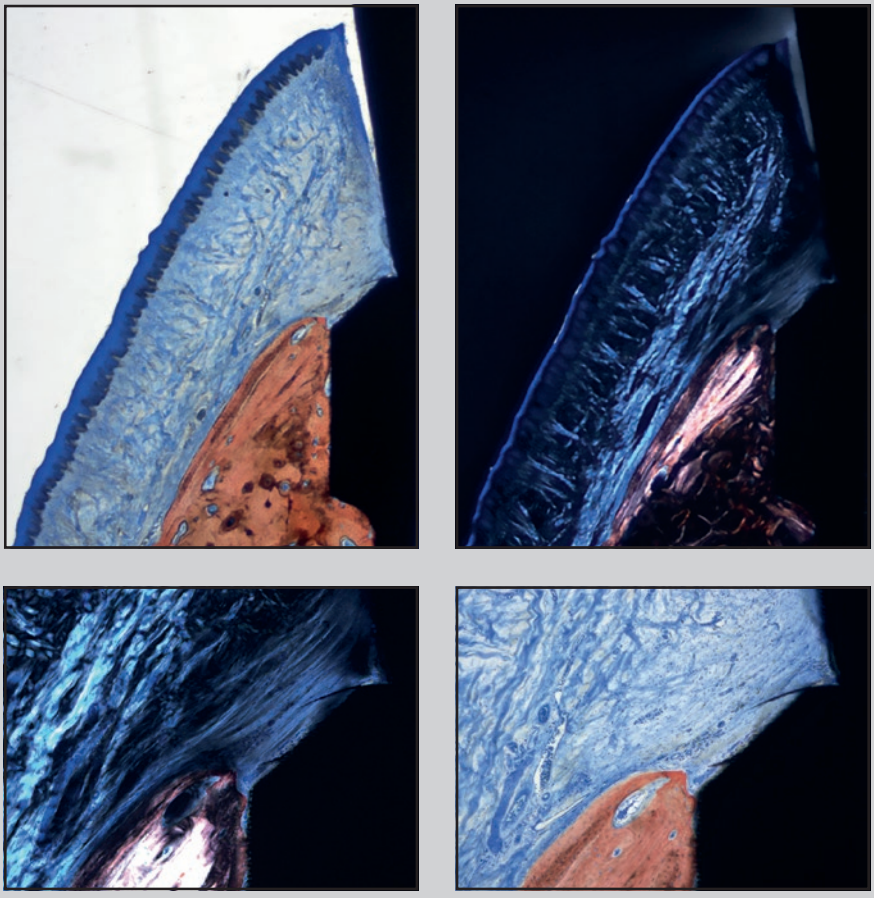

© 2019 BY QUINTESSENCE PUBLISHING CO, INC. PRINTING OF THIS DOCUMENT IS RESTRICTED TO PERSONAL USE ONLY.
NO PART MAY BE REPRODUCED OR TRANSMITTED IN ANY FORM WITHOUT WRITTEN PERMISSION FROM THE PUBLISHER.

The Effect of Laser-Lok Abutments on Fiber Orientation and Buccal Bone Remodeling: A Histomorphometric Study

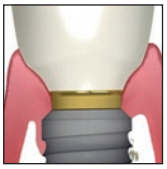

Raquel Rezende Martins de Barros, DDS, PhD[1]
Mauricio Martins Provinciatti, DDS, PhD[2]
Valdir Antonio Muglia, DDS, PhD[2]
Arthur Belém Novaes, Jr, DDS, PhD[1]

The purpose of this study was to evaluate the effect that microgrooved abutments may have on peri-implant tissues. After the flapless extractions of the mandibular premolars of eight dogs, four Laser-Lok implants were placed in each mandibular quadrant, and half of them received laser-microgrooved abutments. A xenograft (MinerOss X, BioHorizons) was used in the gaps. The dogs were euthanized 12 weeks after treatment, and the histomorphometric analysis was performed. Unlike the machined abutments, the microgrooved abutments influenced the orientation of connective tissue fibers, which appeared perpendicularly and adhered to the implant-abutment surfaces, preventing the apical migration of the junctional epithelium. Laser-microgrooved abutments showed superior results.
Int J Periodontics Restorative Dent 2020;40:73–81. doi: 10.11607/prd.4426

[1]Department of Oral and Maxillofacial Surgery and Traumatology and Periodontology, School of Dentistry of Ribeirão Preto, University of São Paulo, São Paulo, SP, Brazil.
[2]Department of Prosthodontics, School of Dentistry of Ribeirão Preto, University of São Paulo, São Paulo, SP, Brazil.

Correspondence to: Dr Arthur B. Novaes, Jr, Department of Oral and Maxillofacial Surgery and Traumatology and Periodontology, Ribeirão Preto Dental School, University of São Paulo, Avenida do Café, S/N, 14040-904. Ribeirão Preto, SP, Brazil. Fax: +55-16-3315-4788. Email: novaesjr@forp.usp.br

Submitted April 17, 2019; accepted June 25, 2019.
©2020 by Quintessence Publishing Co Inc.

The type of implant-abutment connection and its location can act as a modulating variable of the peri-implant bone stability.[1] It was well demonstrated that the microgap formed at the implant-abutment junction is related to microbial contamination[2,3] and micromechanical movements,[4] which directly affect the peri-implant tissue modeling.[3] Studies with platform-switching connections observed that the displacement of the implant-abutment junction (IAJ) towards the center of the implant platform shifts bacterial infiltration, micromovements, and stress away from the crestal bone, therefore with less impact on its resorption.[5,6] Whether the implant installation depth, crestally or subcrestally, can also favor the crestal bone level stability remains questionable. While some studies presented better outcomes placing the implants subcrestally,[7,8] others demonstrated better results with the crestal level of implant insertion.[9,10]

Finally, it has been implied that the modification of the implant collar and abutment surface may affect crestal bone levels.[11] Some studies demonstrated that laser-ablated microgrooved surfaces appear to regulate fibroblastic and osteoblastic behavior, allowing the adhesion of the connective tissue to the implant collar and consequently enhancing the bone level at the critical crestal

© 2019 BY QUINTESSENCE PUBLISHING CO, INC. PRINTING OF THIS DOCUMENT IS RESTRICTED TO PERSONAL USE ONLY.
NO PART MAY BE REPRODUCED OR TRANSMITTED IN ANY FORM WITHOUT WRITTEN PERMISSION FROM THE PUBLISHER.

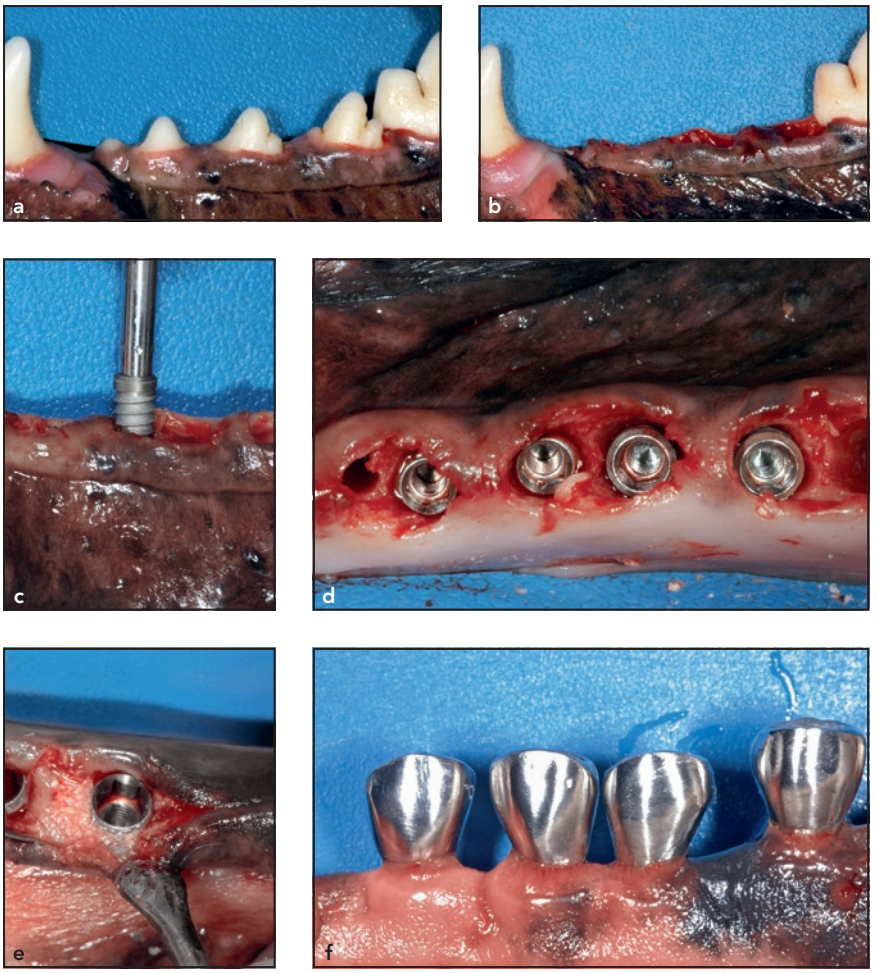

Fig 1 *Mandibular left side* (a) *before, showing the four premolars, and* (b) *after flapless extractions.* (c and d) *Placement of Laser-Lok (BioHorizons) implants.* (e) *The gap between the implant and the buccal bone plate was filled with Miner Oss X (BioHorizons), and* (f) *metallic crowns were placed in the same day, configuring an immediate loading approach.*

region of dental implants.[12,13] Nevins et al[14] showed preliminary results of how the laser microgrooved abutments can also affect peri-implant tissue modeling.

Using histomorphometric analysis, the present preclinical in vivo study primarily evaluated the influence of abutment surface (machined vs laser-microgrooved) on the healing of soft tissue and buccal crestal bone at immediately placed and loaded implants.

Materials and Methods

Study Design

This study was conducted with the approval of the Animal Experimental Ethics Committee (protocol number 2013.1.777.58.1). Eight small beagle dogs, 3 years old and weighing approximately 15 kg, were selected to provide thin buccal bone plates. The protocol follows previous studies from this group.[15–17] Firstly, the dogs were immunized with vaccines, received antiparasitic treatment, and were submitted to dental prophylaxis using ultrasonic points (Cavitron 3000, Dentsply) for removal of dental calculus and bacterial biofilm, as described by Barros et al.[15]

Surgical Procedures

Following anesthesia, eight teeth (four mandibular premolars from each side) were buccolingually sectioned, and the roots were carefully removed, avoiding damage to the alveolar bone walls (Figs 1a and 1b).[15] After tooth extractions, buccal bone thickness was assessed using a surgical micrometer. The distal socket of the second premolar (P2), the mesial and distal sockets of the third premolar (P3), and the mesial socket of the fourth premolar (P4) on both quadrants of the mandible were selected for immediate implant placement (Laser-Lok, BioHorizons) (Figs 1c and 1d). A total of eight implants (Laser-Lok Tapered Internal Plus, BioHorizons) with a 3.8-mm diameter and 9-mm length were placed in each animal (Figs 1e and 1f). All implants were positioned so that their cervical portion remained distant from the buccal bone plate (buccolingual positioning), creating a mean gap of 1.25 mm in this region. This measurement was obtained using a surgical micrometer. With respect to the corono-apical positioning, two installation levels were randomly selected for implants in each side of the mandible: the crestal level (C), where the beginning of the implant

© 2019 BY QUINTESSENCE PUBLISHING CO, INC. PRINTING OF THIS DOCUMENT IS RESTRICTED TO PERSONAL USE ONLY.
NO PART MAY BE REPRODUCED OR TRANSMITTED IN ANY FORM WITHOUT WRITTEN PERMISSION FROM THE PUBLISHER.

collar corresponded exactly to the crestal bone level; and the subcrestal level (SC), in which the implant collar was fully inserted in the prepared bone site (Fig 2). Furthermore, on each side of the mandible, two abutments had their surface treated by the Laser-Lok technology (the same used for the implant collar) while the other two abutments remained untreated (machined). Finally, in each quadrant, two implant sites had their buccal gaps filled with a bone graft (deproteinized bovine bone mineral [MinerOss X, BioHorizons]) (Fig 1e), while the other two sites did not receive grafting and healed only with blood clots. No membranes were associated. Thus, eight study groups were created (G1 to G8). Characteristics of each group are shown in Fig 3.

The different study groups were properly randomized (http://randomization.com) for each animal within the sample in order to vary the different forms of treatment at the different mandibular locations.

In sequence, the wounds were closed with 4-0 absorbable sutures on both sides of the mandible, using mattress or criss-cross sutures to close the margins and aid in retention of coagulum or graft material.[15] All implants were immediately loaded with the installation of metallic crowns (Fig 1f).

Sutures were removed 1 week later, and the animals were euthanized after 15 weeks for a total healing time of 16 weeks. The mandibular quadrants were removed, dissected, cut, and fixed in 10% phosphate buffered formalin (pH 7) and processed for histomorphometry.

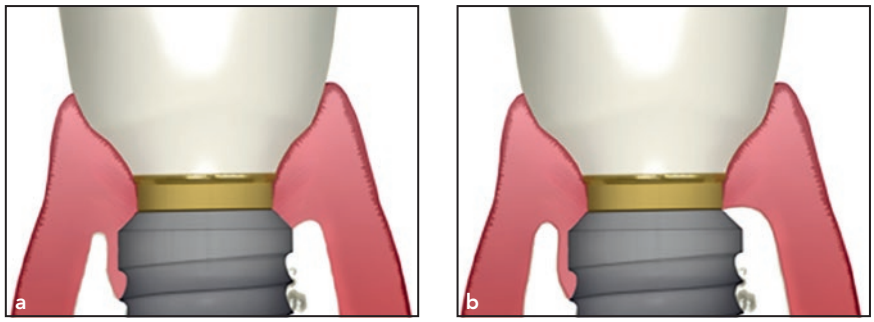

Fig 2 *Schematic illustrations of the two corono-apical implant positions:* (a) *Crestal level, where the beginning of the implant collar corresponds exactly to the crestal bone level, and* (b) *subcrestal level, in which the implant collar is fully inserted in the prepared bone site.*

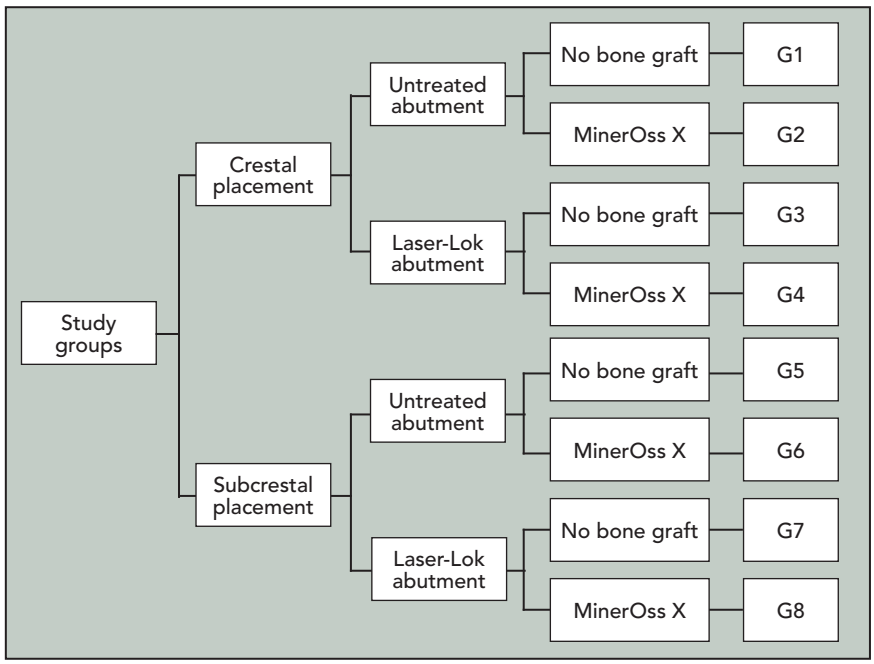

Fig 3 *Characteristics of each study group.*

Histomorphometric Analysis

Buccolingual longitudinal histologic sections from each implant were analyzed on a Leica DM LB2 microscope outfitted with a Leica DFC310 FX digital camera (Leica Microsystems). The images were analyzed through the Leica Application Suite version 4.1 by a single examiner with no knowledge of the experimental groups, as in Barros et al.[15]

Hard tissue evaluation was performed as described by Suaid et al[16] (Fig 4).

In the soft tissue evaluation, the positioning of the junctional epithelium (JE) was investigated as a vertical line measurement (in millimeters) from the most apical part of the JE to the IAJ (Figs 5a and 5b). Positive numbers indicate that the apical migration of the JE ended above the IAJ, but negative numbers signify

© 2019 BY QUINTESSENCE PUBLISHING CO, INC. PRINTING OF THIS DOCUMENT IS RESTRICTED TO PERSONAL USE ONLY.
NO PART MAY BE REPRODUCED OR TRANSMITTED IN ANY FORM WITHOUT WRITTEN PERMISSION FROM THE PUBLISHER.

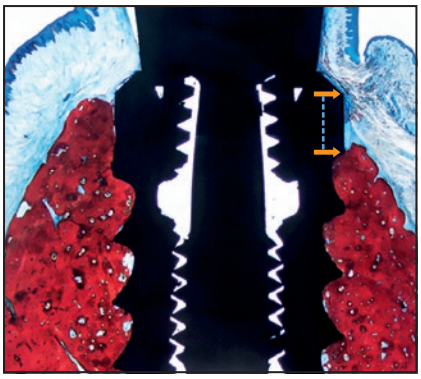

Fig 4 *The bone level* (dashed blue line) *was the linear vertical measurement from the implant shoulder* (top arrow) *to the first bone-to-implant contact* (bottom arrow) *in both buccal and lingual sides.*

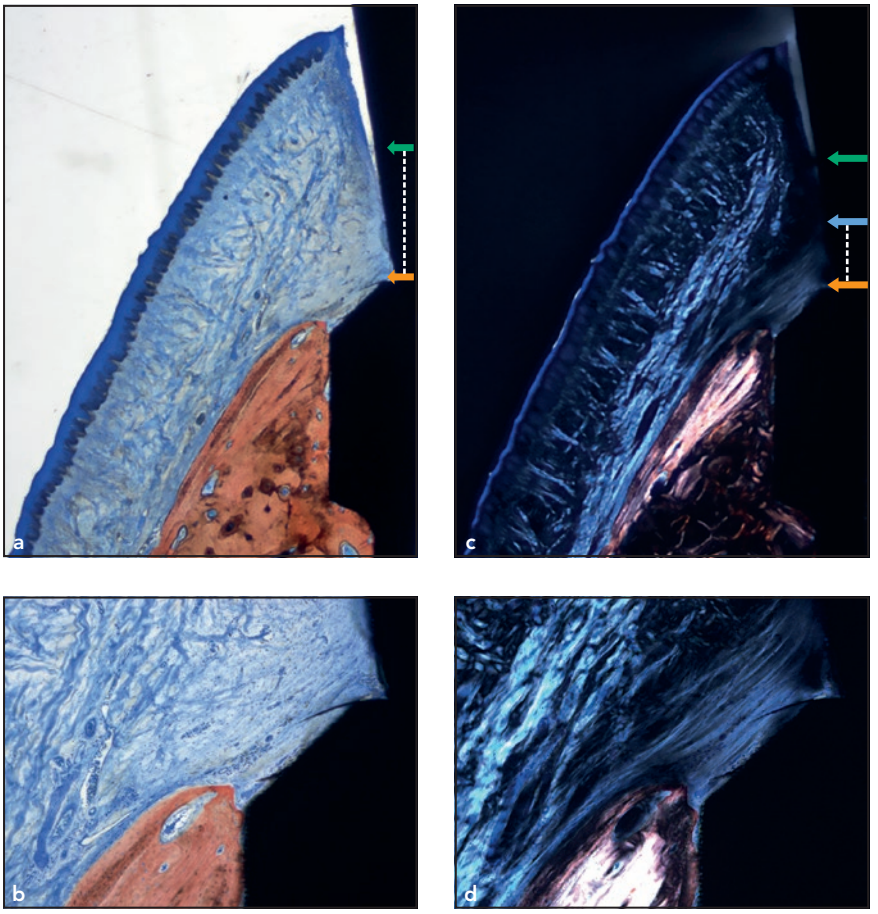

Fig 5 *Histologic image of a G4 specimen (Alizarin red stain, ×2.5 magnification).* (a) *The apical migration* (dashed white line) *of the junctional epithelium (JE) was investigated through a linear vertical measurement from the bottom of the JE* (green arrow) *to the implant abutment junction (IAJ; orange arrow).* (b) *Higher magnification (×10) shows excellent level of the crestal bone in relation to the IAJ.* (c) *Using the polarized light, the supracrestal connective tissue fibers barrier* (dashed white line) *was measured from the IAJ (orange arrow) to the final fiber attachment* (blue arrow); the green arrow points to the JE; (d) *Higher magnification (×10) shows the oblique orientation of the connective tissue fibers, functionally inserted.*

that the JE migration reached the implant body region, remaining below the IAJ.

The barrier of supracrestal connective tissue fibers was measured when present (Fig 5c). The orientation of these fibers in relation to the abutment surface was described as perpendicular, oblique, or parallel in the different experimental groups. They were better observed using polarized light in the histologic sections (Figs 5c and 5d).

Statistical Analysis

The investigated parameters were described in mean values, median values, and standard deviations. Nonparametric analysis of variance (Kruskal-Wallis test) with Dunn's multiple comparisons test was used for intergroup comparisons, while Wilcoxon matched pairs test was used for intragroup analysis. The statistical software used for the analysis was the GraphPad Instat (GraphPad Software) with a 95% confidence level.

Results

Clinical Analysis

Data regarding the buccal bone crest width and the gap between the implant shoulder and the buccal bone plate showed equivalence between the groups at baseline (Table 1).

A thin buccal bone plate was a common characteristic between the groups. Quantitatively, the buccal bone thickness means varied from

© 2019 BY QUINTESSENCE PUBLISHING CO, INC. PRINTING OF THIS DOCUMENT IS RESTRICTED TO PERSONAL USE ONLY.
NO PART MAY BE REPRODUCED OR TRANSMITTED IN ANY FORM WITHOUT WRITTEN PERMISSION FROM THE PUBLISHER.

Table 1 Baseline Clinical Measurements (mm) of BBCW and GAP in the Experimental Groups

	G1	G2	G3	G4	G5	G6	G7	G8	*P*
BBCW									.7786
Mean	0.75	0.87	0.83	0.87	0.93	0.81	1	1	
SD	0.26	0.44	0.41	0.35	0.41	0.37	0.26	0.26	
Median	0.75	0.75	1	1	1	0.75	1	1	
GAP									.5343
Mean	1.28	1.16	1.25	1.38	1.18	1.16	1.38	1.25	
SD	0.18	0.31	0.31	0.34	0.15	0.16	0.30	0.16	
Median	1.20	1.20	1.20	1.20	1.20	1.20	1.35	1.20	

BBCW = buccal bone crest width; GAP = gap between the implant shoulder and the buccal bone plate; SD = standard deviation.
Kruskal-Wallis test (non-parametric analysis of variance) was used to calculate *P* values (intergroup analysis).
$P < .05$ was considered statistically significant.

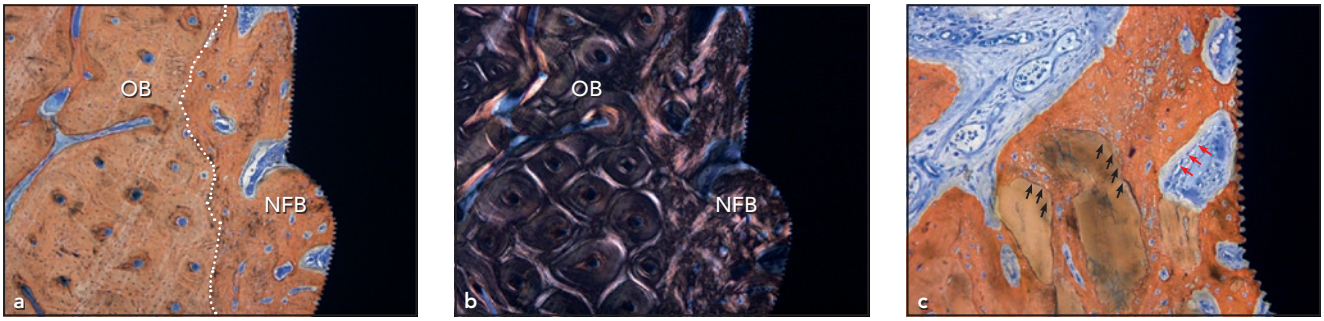

Fig 6 (a and b) *Histologic image of a G7 specimen (Alizarin red stain, ×10 magnification).* (a) *The 'old bone' (OB) was evidenced as a lamellar bone area, while the newly formed bone area (NFB, separated by the dotted line) was characterized as a parallel-fibered bone with areas of interlaced fibers.* (b) *In the polarized light, the areas occupied by the different bone types (OB, NFB) are easily identified by the orientation of the collagen fibers.* (c) *Histologic image of a G4 specimen (Alizarin red stain, ×20 magnification). Observe the residual graft particles* (black arrows) *present in the gap area, in close contact to the newly formed bone, evidencing a good osseointegration rate. Areas of osteoid matrix paved with osteoblasts* (red arrows) *were also observed.*

0.75 mm to 1 mm in the experimental groups.

Histologic Analysis

Light microscopy analysis evidenced early osseointegration of the implants in general. Significant bone-to-implant contact and bone density were noted along the extension of the implant textured surface after 16 weeks of healing. In all specimens, the buccal bone plates were significantly thinner than the lingual bone plates.

As is common, signs of immaturity were noted, constituting the bone adjacent to the implant surface, which was easily distinguished from the parent lamellar bone (older bone) that appeared distant from the implant surface (Figs 6a and 6b). The orientation of the collagen fibers, the number of osteocytes, and the diameter of the osteocyte lacunae were different between the bone types (Figs 6a and 6b). As defined in Suaid et al,[16] a newly formed structure was characterized as a parallel fibered bone with a lamellar pattern, but a tissue with interlaced fibers characterizing woven bone was present in some areas. In both types of newly formed bone, a higher number of osteocytes inside wide lacunae were observed when compared to the older bone. In some regions, a line of osteoblasts was seen, paving an osteoid matrix and constituting an active point of bone formation (Fig 6c).

© 2019 BY QUINTESSENCE PUBLISHING CO, INC. PRINTING OF THIS DOCUMENT IS RESTRICTED TO PERSONAL USE ONLY.
NO PART MAY BE REPRODUCED OR TRANSMITTED IN ANY FORM WITHOUT WRITTEN PERMISSION FROM THE PUBLISHER.

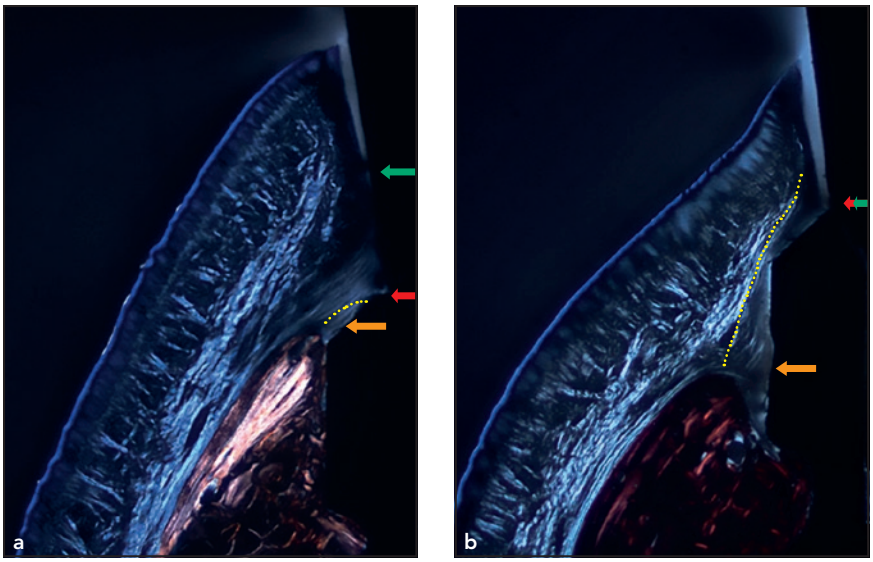

Fig 7 (a) *A functionally oriented supracrestal connective tissue barrier* (yellow dotted line) *was evidenced in microgrooved abutment groups, preventing the apical migration of the junctional epithelium* (distance between green and red arrows) *and crestal resorption* (orange arrow). (b) *In the machined abutment groups, the connective tissue fibers ran parallel to the abutment and implant surfaces, not attached to them. Note the imposition of a long junctional epithelium* (green and red arrow at the same level) *and crestal bone resorption* (distance between red and orange arrows).

Table 2 Histomorphometric Buccal Bone Resorption (Linear Vertical Measurement from the IS to the First BIC)

	G1	G2	G3	G4	G5	G6	G7	G8	*P*
Mean, mm	1.22[a]	1.11[b]	0.93	0.66[abcd]	1.16[c]	1.13[d]	0.94	0.89	.048[abcd]
SD, mm	0.52	0.29	0.56	0.25	0.31	0.32	0.38	0.23	
Median, mm	0.96	1.10	0.85	0.70	1.08	1.07	0.83	0.95	

IS = implant shoulder; BIC = bone-to-implant contact; SD = standard deviation.
Repeated superscript letters within a row indicate intergroup comparisons with statistical significance.
Kruskal-Wallis test (non-parametric analysis of variance) with Dunn's multiple comparisons test was used to calculate *P* values (intergroup analysis). $P < .05$ was considered statistically significant.

Eventually, in the grafted groups, residual particles of the xenograft were seen near the implant surface, within the original gap at the buccal side; however, these particles appeared extremely integrated to the recently formed bone (Fig 6c).

Examining the peri-implant soft tissues, the epithelial barrier was composed of sulcular epithelium and JE (Fig 5a). A functionally oriented supracrestal connective tissue barrier was evidenced in the treated abutment groups, independently of the gap defect augmentation and implant placement depth (Fig 5c). In 25% of the G3, G4, G7, and G8 specimens (microgrooved abutments), the connective tissue fibers were seen perpendicular to the microgrooved band of the abutment; in the other 75%, they appeared in an oblique orientation, both of them preventing the apical migration of the JE (Figs 5d and 7a).

In all the specimens of the untreated abutment groups (G1, G2, G5, and G6), the apical migration of the JE was evidenced, and the connective tissue fibers were seen parallel to the abutment and implant surfaces, not forming an effective barrier above the crestal bone as seen in the other groups (Fig 7b).

Histomorphometric Analysis

Hard Tissue Assessments

In the present study, the groups treated with Laser-Lok abutments and MinerOss X (G4 and G8) exhibited better histomorphometric results in all parameters (Table 2).

Soft Tissue Assessments

Apical migration of the junctional epithelium was frequently observed in groups with untreated abutments, but the same did not occur with the microgrooved abutments; the differences were statistically significant (Fig 8). No statistically significant

© 2019 BY QUINTESSENCE PUBLISHING CO, INC. PRINTING OF THIS DOCUMENT IS RESTRICTED TO PERSONAL USE ONLY.
NO PART MAY BE REPRODUCED OR TRANSMITTED IN ANY FORM WITHOUT WRITTEN PERMISSION FROM THE PUBLISHER.

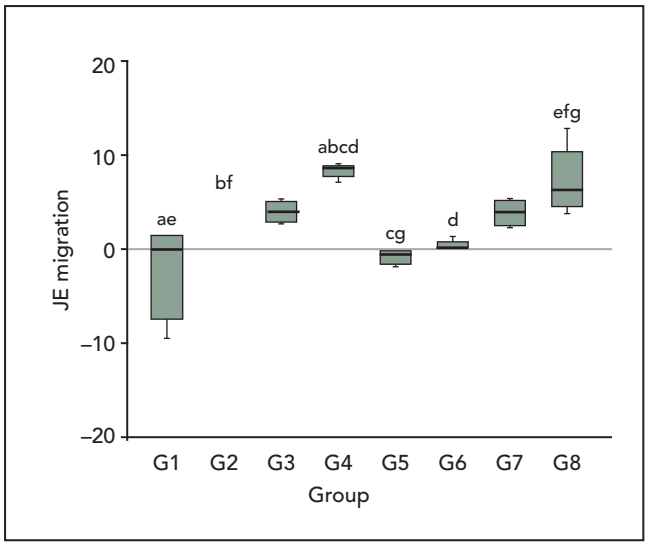

Fig 8 *Histomorphometric soft tissue evaluation between the experimental groups represented by medians and interquartile range. Junctional epithelium (JE) migration was evaluated as a linear vertical measurement (in millimeters) from the bottom of the JE to the implant abutment junction (IAJ). Kruskal-Wallis test (non-parametric analysis of variance) with Dunn's multiple comparisons test was used for intergroup comparisons. Repeated superscript letters within a row indicate intergroup comparisons with statistical relevance. P < .01 for G1 × G4, G2 × G4, and G4 × G5. P < .05 for G4 × G6, G1 × G8, G2 × G8, and G5 × G8.*

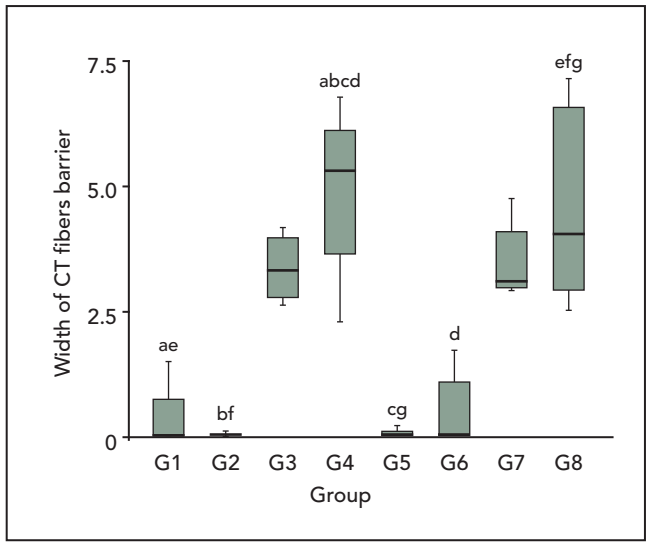

Fig 9 *Histomorphometric soft tissue evaluation between the experimental groups represented by medians and interquartile range. When present, widths of supracrestal connective tissue (CT) fibers barriers were measured in millimeters. Kruskal-Wallis test (non-parametric analysis of variance) with Dunn's multiple comparisons test was used for intergroup comparisons. Repeated superscript letters within a row indicate intergroup comparisons with statistical relevance. P < .01 for G1 × G4, G2 × G4, and G4 × G5. P < .05 for G4 × G6, G1 × G8, G2 × G8, and G5 × G8.*

differences were obtained between crestal and subcrestal groups.

The formation of a supracrestal connective tissue barrier was another evaluated parameter for soft tissues. In the microgrooved-abutment groups, a zone of connective tissue fibers was observed, functionally oriented to the abutments. This was not seen on the smooth abutments, where the connective tissue fibers were seen parallel to the abutment and implant surfaces, not effectively forming a barrier to the apical migration of the junctional epithelium. The differences were statistically significant in favor of the microgrooved abutments, but again, no differences were found between crestal and subcrestal groups (Fig 9).

Discussion

Marginal bone preservation is of great importance for the success and esthetics of implants placed in fresh extraction sockets. With this in mind, the present study investigated some variables that can potentially modulate the remodeling of peri-implant bone, such as the modification of the abutment surface with the laser-microgrooving technology, filling the gap between the buccal bone plate and the implant with a new xenograft material, and different implant positioning depths.

The present results demonstrated that both laser-microgrooved abutments and gap augmentation with MinerOss X, especially around crestally placed implants, achieved significantly better performance in general, not exclusively in the maintenance of the buccal crestal bone height (Table 2). The literature on this type of abutment modification is still very scarce. Nevins et al[14] also compared laser-microgrooved

© 2019 BY QUINTESSENCE PUBLISHING CO, INC. PRINTING OF THIS DOCUMENT IS RESTRICTED TO PERSONAL USE ONLY.
NO PART MAY BE REPRODUCED OR TRANSMITTED IN ANY FORM WITHOUT WRITTEN PERMISSION FROM THE PUBLISHER.

and traditional machined abutments, demonstrating a significant improvement of the proximal peri-implant hard and soft tissue healing in the group with treated abutments; different from the present study, the histologic specimens were analyzed in mesial-distal sections. In a histologic case report by Nevins et al[17] that utilized laser-microgrooved abutments in humans, a similar outcome was found. Iglhaut et al,[18] corroborating these findings, showed histomorphometrically that abutments with either partially or full laser-microgrooved margins enhanced subepithelial connective tissue attachment and better preserved the crestal bone levels when compared to machined surface margins. The present results are in accordance with the aforementioned, regardless of the study's more-challenging methodology, such as immediate placement and loading of the implants as well as evaluating the specimens in buccolingual sections, where the crestal bone levels are more prone to resorption. The immediate prosthesis and its emergence profile will guide epithelial and connective tissue healing, mimicking the clinical situation somewhat better. In terms of osseointegration levels, the bone-to-implant contact results in the present study were also better for the laser-microgrooved abutment groups, particularly in the grafted groups where the implants were placed crestally (G4). The bone density assessments also revealed the same trend, showing that abutment modifications may also benefit the bone quality around the implants. A possible explanation for these findings was given by Nevins et al,[14] who showed that this specific modification of the abutment surface provided an improved microenvironment for a direct fibrocollagenous attachment, which potentially limits the apical epithelial migration, thus preventing crestal bone loss. In addition, direct attachment of connective tissues to the abutment surface may potentially diminish the microbial contamination's negative impact on the IAJ, favoring the marginal bone. The present results of peri-implant soft tissues confirmed this hypothesis. Two different outcomes were systematically observed when the groups were separated by the treatment of the abutment surface. A supracrestal connective tissue band was seen in the groups with laser-microgrooved abutments, where the fibers were oriented perpendicular or obliquely to the abutment surface. It is reasonable to suggest that they constituted a physiologic barrier for the epithelial downgrowth once the apical JE appeared in a coronal position, in relation to the IAJ. Differently, the connective tissue fibers appeared parallel to the abutment and implant surfaces in the machined abutment groups; moreover, the imposition of a long JE was found in these groups, explaining the high levels of crestal bone resorption (Fig 7).

Previous studies[12,18] that used the same technology to modify the implant collars reported that the laser-microgrooved surfaces can influence cell behavior, preferentially guiding specific cell types. It was explained that the perpendicular orientation of the connective tissue fibers on the surface of the microgrooved group can be expected to prevent epithelial downgrowth and saucerization around the implants.[19]

Limitations of this study include the number of animals, which is limited by the Ethics Committee and costs. As with all animal studies, direct translation to humans should be done with caution.

Conclusions

The present study demonstrated that laser-microgrooved abutments placed in sockets with grafting of buccal gap defects may positively and significantly affect the establishment soft tissues with functionally oriented collagen fibers. These results appeared to be related to better levels of buccal bone height around implants that were immediately placed and loaded during flapless surgeries, more expressively when the Laser-Lok platform-switched implants were placed crestally.

Acknowledgments

The authors thank the National Council for Scientific and Technological Development (CNPq; process number 162546/2013-0) for the scholarship that supported Dr Barros, the State of São Paulo Research Foundation (FAPESP) for the financial support of this study (process number 2013/24324-0), and BioHorizons (Birmingham, Alabama) for the donation of the implants and surgical and graft materials used in this study. The authors also thank Adriana Luisa Gonçalves

© 2019 BY QUINTESSENCE PUBLISHING CO, INC. PRINTING OF THIS DOCUMENT IS RESTRICTED TO PERSONAL USE ONLY.
NO PART MAY BE REPRODUCED OR TRANSMITTED IN ANY FORM WITHOUT WRITTEN PERMISSION FROM THE PUBLISHER.

de Almeida, laboratory technician of the Department of Oral and Maxillofacial Surgery and Traumatology and Periodontology at the Ribeirão Preto Dental School, University of São Paulo, for her kindly help with the histomorphometric analysis. The authors certify that they have no affiliations with or involvement in any organization or entity with any financial interest or nonfinancial interest in the subject matter or materials discussed in this manuscript.

References

1. Schwarz F, Hegewald A, Becker J. Impact of implant-abutment connection and positioning of the machined collar/microgap on crestal bone level changes: A systematic review. Clin Oral Implants Res 2014;25:417–425.
2. Broggini N, McManus LM, Hermann JS, et al. Peri-implant inflammation defined by the implant-abutment interface. J Dent Res 2006;85:473–478.
3. Covani U, Marconcini S, Crespi R, Barone A. Bacterial plaque colonization around dental implant surfaces. Implant Dent 2006;15:298–304.
4. Hermann JS, Schoolfield JD, Schenk RK, Buser D, Cochran DL. Influence of the size of the microgap on crestal bone changes around titanium implants. A histometric evaluation of unloaded nonsubmerged implants in the canine mandible. J Periodontol 2001;72;1372–1383.
5. Lazzara RJ, Porter SS. Platform switching: A new concept in implant dentistry for controlling postrestorative crestal bone levels. Int J Periodontics Restorative Dent 2006;26:9–17.
6. Canullo L, Fedele GR, Iannello G, Jepsen S. Platform switching and marginal bone-level alterations: The results of a randomized-controlled trial. Clin Oral Implants Res 2010;21:115–121.
7. Weng D, Nagata MJ, Bell M, Bosco AF, de Melo LG, Richter EJ. Influence of microgap location and configuration on the periimplant bone morphology in submerged implants. An experimental study in dogs. Clin Oral Implants Res 2008;19:1141–1147.
8. Calvo-Guirado JL, Gomez Moreno G, Aguilar-Salvatierra A, Mate Sanchez de Val JE, Abboud M, Nemcovsky CE. Bone remodeling at implants with different configurations and placed immediately at different depth into extraction sockets. Experimental study in dogs. Clin Oral Implants Res 2015;26:507–515.
9. Cochran DL, Bosshardt DD, Grize L, et al. Bone response to loaded implants with non-matching implant-abutment diameters in the canine mandible. J Periodontol 2009;80:609–617.
10. Becker J, Ferrari D, Mihatovic I, Sahm N, Schaer, A, Schwarz F. Stability of crestal bone level at platform-switched nonsubmerged titanium implants: A histomorphometrical study in dogs. J Clin Periodontol 2009;36:532–539.
11. Hsu YT, Chan HL, Rudek I, et al. Comparison of clinical and radiographic outcomes of platform-switched implants with a rough collar and platform-matched implants with a smooth collar: A 1-year randomized clinical trial. Int J Oral Maxillofac Implants 2016;31:382–390.
12. Weiner S, Simon J, Ehrenberg DS, Zweig B, Ricci JL. The effects of laser microtextured collars upon crestal bone levels of dental implants. Implant Dent 2008;17:217–228.
13. Nevins M, Nevins ML, Camelo M, Boyesen JL, Kim DM. Human histologic evidence of a connective tissue attachment to a dental implant. Int J Periodontics Restorative Dent 2008;28:111–121.
14. Nevins M, Kim DM, Jun SH, Guze K, Schupbach P, Nevins ML. Histologic evidence of a connective tissue attachment to laser microgrooved abutments: A canine study. Int J Periodontics Restorative Dent 2010;30:245–255.
15. Barros RRM, Novaes AB Jr, de Carvalho JP, de Almeida ALG. The effect of a flapless alveolar ridge preservation procedure with or without a xenograft on buccal bone crest remodeling compared by histomorphometric and microcomputed tomographic analysis. Clin Oral Implants Res 2017;28:938–945.
16. Suaid FA, Novaes AB Jr, Queiroz AC, Muglia VA, Almeida AL, Grisi MF. Buccal bone plate remodeling after immediate implants with or without synthetic bone grafting and flapless surgery: A histomorphometric and fluorescence study in dogs. Clin Oral Implants Res 2014;25:e10–e21.
17. Nevins M, Camelo M, Nevins ML, Schupbach P, Kim DM. Connective tissue attachment to laser-microgrooved abutments: A human histologic case report. Int J Periodontics Restorative Dent 2012;32:385–392.
18. Iglhaut G, Becker K, Golubovic V, Schliephake H, Mihatovic I. The impact of dis-/reconnection of laser microgrooved and machined implant abutments on soft- and hard-tissue healing. Clin Oral Implants Res 2013;24:391–397.
19. Shin SY, Han DH. Influence of a microgrooved collar design on soft and hard tissue healing of immediate implantation in fresh extraction sites in dogs. Clin Oral Implants Res 2010;21:804–814.

© 2019 BY QUINTESSENCE PUBLISHING CO, INC. PRINTING OF THIS DOCUMENT IS RESTRICTED TO PERSONAL USE ONLY.
NO PART MAY BE REPRODUCED OR TRANSMITTED IN ANY FORM WITHOUT WRITTEN PERMISSION FROM THE PUBLISHER.